1 **Thiostrepton hijacks pyoverdine receptors to inhibit growth of *Pseudomonas aeruginosa***

2 Michael R. Ranieri, Derek C. K. Chan, Luke Yaeger, Madeleine Rudolph, Sawyer Karabelas-Pittman,
3 Hamdi Abdo, Jessica Chee, Hanjeong Harvey, Uyen Nguyen, and Lori L. Burrows.

4 Department of Biochemistry and Biomedical Sciences, and the Michael G. DeGroote Institute for
5 Infectious Diseases Research, McMaster University, Hamilton, ON

6

7 **Running title:** Thiostrepton inhibits growth of *Pseudomonas aeruginosa*

8

9 **Keywords:** antibiotic, thiopeptide, iron, siderophore, gram negative

10

11 ***Correspondence to**:

12 Dr. Lori L. Burrows

13 4H18 Health Sciences Centre, 1280 Main St. West,

14 Hamilton, ON L8S 4K1 Canada

15 Tel: 905-525-9140 x 22029 Fax: 905-522-9033 Email: burrowl@mcmaster.ca

16

ABSTRACT

Pseudomonas aeruginosa is a biofilm-forming opportunistic pathogen and intrinsically resistant to many antibiotics. In a high-throughput screen for molecules that modulate biofilm formation, we discovered that the thiopeptide antibiotic, thiostrepton (TS) - considered inactive against Gram-negative bacteria - stimulated *P. aeruginosa* biofilm formation in a dose-dependent manner. This phenotype is characteristic of exposure to antimicrobial compounds at sub-inhibitory concentrations, suggesting that TS was active against *P. aeruginosa.* Supporting this observation, TS inhibited growth of a panel of 96 multidrug-resistant (MDR) *P. aeruginosa* clinical isolates at low micromolar concentrations. TS also had activity against *Acinetobacter baumannii* clinical isolates. Expression of Tsr - a 23S rRNA-modifying methyltransferase - in trans conferred TS resistance, confirming that the drug acted via its canonical mode of action, inhibition of ribosome function. Deletion of oligopeptide permease systems used by other peptide antibiotics for uptake failed confer TS resistance. TS susceptibility was inversely proportional to iron availability, suggesting that TS exploits uptake pathways whose expression is increased under iron starvation. Consistent with this finding, TS activity against *P. aeruginosa* and *A. baumannii* was potentiated by FDA-approved iron chelators deferiprone and deferasirox. Screening of *P. aeruginosa* mutants for TS resistance revealed that it exploits pyoverdine receptors FpvA and FpvB to cross the outer membrane. Our data show that the biofilm stimulation phenotype can reveal cryptic sub-inhibitory antibiotic activity, and that TS has activity against select multidrug resistant Gram-negative pathogens under iron-limited growth conditions, similar to those encountered at sites of infection.

INTRODUCTION

Bacterial pathogens are rapidly evolving resistance to available antibiotics, creating an urgent need for new therapies. Gram-negative bacteria are particularly challenging to treat because their outer membranes limit the access of many drugs to intracellular targets (1). Resistance arises when bacteria accumulate target mutations, acquire specific resistance determinants, increase drug efflux, and/or enter antibiotic-tolerant dormant or biofilm modes of growth (2). Biofilms consist of surface-associated bacteria surrounded by self-produced extracellular polymeric substances (EPS). Biofilm architecture allows for development of phenotypic heterogeneity that leads to variations in susceptibility as well as the formation of drug-tolerant persister cells (3). Approaches with the potential to preserve current antibiotics include combining them with biofilm inhibitors, resistance blockers (e.g. ampicillin with

clavulanic acid or piperacillin with tazobactam), efflux inhibitors (e.g. PAβN), outer membrane permeabilizers, or coupling them to molecules such as siderophores that are actively imported, so-called Trojan horses (4).

Among the bacterial pathogens deemed most problematic by the World Health Organization is the Gram-negative opportunist, *Pseudomonas aeruginosa* (5). It infects immunocompromised patients – particularly those with medical devices – and is a major problem for people with severe burns or cystic fibrosis (6). It is intrinsically resistant to many antibiotics and readily forms biofilms, further enhancing its ability to evade therapy (7). The low permeability of its outer membrane and expression of multiple efflux pumps that extrude a wide variety of substrates, coupled with its propensity to form biofilms, limits the repertoire of effective anti-*Pseudomonas* antibiotics (8-10). Here with the initial aim of identifying potential modulators of *P. aeruginosa* biofilm formation, we screened a collection of bioactive molecules including previously FDA-approved off-patent drugs. During this work, we identified several molecules that stimulated biofilm formation beyond our arbitrary cutoff of 200% of the vehicle control. Investigation of one such stimulatory compound, thiostrepton (TS), revealed that it had low micromolar activity against *P. aeruginosa* in minimal medium. Through a series of investigations, we showed that TS gains access to its ribosomal targets by exploiting iron limitation-dependent uptake pathways. These data show that the biofilm stimulation phenotype can reveal cryptic antibiotic activity when concentrations are too low (or growth conditions not conducive) to inhibit growth.

RESULTS

Thiostrepton stimulates *P. aeruginosa* biofilm formation

We used a previously described *P. aeruginosa* biofilm assay (11) to screen a bespoke collection of 3921 bioactive molecules that includes ~1100 FDA-approved, off-patent drugs and antibiotics (12). The molecules were screened in duplicate at 10 μM in a dilute growth medium consisting of 10% lysogeny broth (LB), 90% phosphate buffered saline (henceforth, 10:90) to identify molecules capable of modulating biofilm formation. This medium was chosen to minimize the amount of biofilm formed in the presence of the vehicle control, so that molecules that stimulated biofilm formation could be more easily identified. The hits were divided into planktonic growth inhibitors (60 compounds), biofilm inhibitors (defined as those resulting in ≤50% of vehicle control biofilm, 8 compounds), or biofilm stimulators (those resulting in ≥200% of vehicle-treated control biofilm, 60 compounds) (**Supplementary Table S1**). The hit rate of ~3% was relatively high for a primary screen, but all the molecules in this

curated collection have biological activity. The hits belonged to a variety of chemical classes and included drugs with nominally eukaryotic targets.

Multiple studies showed that sub-inhibitory concentrations of antibiotics from a variety of classes and with different mechanisms of action (MOA) stimulate *P. aeruginosa* biofilm formation, although the specific pathways underlying this response remain unclear (13-18). Among the molecules in our screen that stimulated biofilm formation was the thiopeptide antibiotic, thiostrepton (TS; **Fig 1A**). This response intrigued us because TS is considered ineffective against Gram-negative bacteria due to the impermeability of the outer membrane (OM) to large hydrophobic compounds (19, 20). In dose-response experiments in 10:90 medium, biofilm levels increased while planktonic cell density decreased with increasing TS concentrations to 10 µM (17 µg/ml), the maximum that could be tested due to its limited solubility (**Fig 1B)**.

Growth in minimal media increases susceptibility of *P. aeruginosa* to TS

Environmental conditions can modulate the expression or essentiality of antibiotic targets or alter the availability of particular nutrients (21), leading to changes in susceptibility. We hypothesized that the biofilm response of *P. aeruginosa* to TS may be the result of nutrient deficiency in 10:90, which was more limiting to *P. aeruginosa* growth than M9 minimal medium (**Supplementary Fig S1**). Growth in Vogel Bonner Minimal Media (VBMM) in the absence of TS was similar to that in 10:90 (**Supplementary Fig S1**) but in the presence of TS, planktonic cell density decreased to below the level of detection at concentrations above ~1.25µM (**Fig 1C**). These data suggested that nutrient limitation enhances susceptibility of *P. aeruginosa* to TS.

The ribosomal methyltransferase Tsr protects *P. aeruginosa* against TS

The established MOA for TS is inhibition of protein translation through direct binding to bacterial ribosomes (22). However, because TS also has anti-parasitic and anti-neoplastic activities (23, 24) we considered the possibility that it might inhibit *P. aeruginosa* growth in a novel way. To validate the MOA, we expressed a resistance gene, *tsr,* from a plasmid in *P. aeruginosa* strains PAO1 and PA14. *tsr* encodes a 23s rRNA methyltransferase, used by TS producer *Streptomyces azureus* to prevent self-intoxication (25). Tsr methylates the conserved A1067 residue of 23s rRNA, impairing binding of TS to its target (26). Expression of *tsr* in trans increased TS resistance of both PAO1 and PA14 compared to vector-only controls (**Fig 2**). PAO1 was resistant up to the maximum soluble TS concentration of 10 µM, while resistance of PA14 was significantly increased compared to control, although not to the same

extent as PAO1. These results suggest that TS inhibits growth via its canonical MOA of ribosome binding, implying that it can cross the *P. aeruginosa* OM to access the bacterial cytoplasm.

TS susceptibility increases in the presence of iron chelators

To understand the reason for increased TS susceptibility of *P. aeruginosa* in VBMM compared to 10:90, we considered the differences in nutrient availability between the two media types. The primary carbon source in 10% LB is amino acids (27) while the carbon source in VBMM is citrate (28). Citrate can chelate divalent cations including calcium and magnesium, which are important for OM integrity. We hypothesized that this chelation effect may increase OM permeability. To stabilize the OM, we repeated the dose response assay in VBMM supplemented with 100 mM $MgCl_2$ but saw no effect on susceptibility (**Supplementary Fig S2A**). Since TS is a thiopeptide, we next hypothesized that amino acid limitation during growth in VBMM may increase uptake of TS, leading to growth inhibition. To test this, we supplemented VBMM with 0.1% casamino acids, but saw no change in TS susceptibility (**Supplementary Fig 2B**). Further, simultaneous deletion of components of the Opp (Npp) peptide transport system, exploited by other peptide antibiotics for entry (29, 30), and a homologous system, Spp, had no effect on TS susceptibility (**Supplementary Fig S2C**).

We next considered that VBMM was more iron-limited than 10:90, which contains trace iron from yeast extract and peptone. Under iron limitation, bacteria secrete siderophores into the extracellular milieu to scavenge the metal. Specialized receptors then transport siderophore-iron complexes back into the cell. Some antimicrobials, including sideromycins, pyocins, and bacteriocins, use siderophore receptors to access intracellular targets (31-34), and we hypothesized that TS may use this strategy. We compared *P. aeruginosa* PAO1 grown in 10:90 with increasing concentrations of TS alone (**Fig 3A**) or with 0.1µM EDDHA, a membrane-impermeable iron chelator (35) (**Fig 3B**). Addition of EDDHA shifted biofilm stimulation and growth inhibition to lower concentrations of TS compared to 10:90 alone. Supplementation of 10:90 plus 0.1µM EDDHA with 100µM $FeCl_3$ increased planktonic cell density and reduced biofilm stimulation (**Fig 3C**). These data suggest that TS susceptibility is inversely proportional to iron availability, and that TS may exploit siderophore receptors to cross the OM of *P. aeruginosa*.

The poor solubility of TS has hampered its development as a therapeutic, but these data suggested that its effective concentration could be reduced in the presence of iron chelators. We tested the FDA-approved iron chelators deferiprone (DFP) and deferasirox (DSX) for potential synergy with TS.

Checkerboard assays revealed that while neither chelator had activity against *P. aeruginosa* on its own, both potentiated TS activity (**Fig 3DE**) at concentrations well below those used to safely treat patients, up to 28 mg/kg/day for DSX or 99 mg/kg/day for DFP (36).

TS hijacks pyoverdine receptors FpvA and FpvB

To identify the route of iron-limitation dependent TS entry into *P. aeruginosa*, we tested the susceptibility of mutants from the ordered PA14 transposon library (37) that had insertions in genes encoding known siderophore receptors, as well as mutants with insertions in uncharacterized OM proteins with homology to siderophore receptors. In VBMM, most mutants had an IC_{50} of 0.16 µM (0.26 µg/ml), similar to the parental strain (**Table 1**). In contrast, an *fpvA* mutant, encoding the type I pyoverdine receptor, had an IC_{50} of 3.5 µM. Growth inhibition was still observed at the highest TS concentrations, indicating that the *fpvA* mutant remained partially susceptible. *P. aeruginosa* encodes two type I pyoverdine receptors, FpvA and FpvB, with ~39% amino acid identity (71% similarity). The *fpvB* mutant was also less susceptible to TS than the parent strain, with an IC_{50} of 1 µM. Based on these patterns of susceptibility, we speculated that TS may use both FpvA and FpvB, but that FpvA was the preferred receptor. When we deleted *fpvA* in the *fpvB* background, the double mutant was more resistant to TS than the single mutants, with an IC_{50} of 6.3 µM (**Table 1**). Complementation of the *fpvAB* mutant with *fpvB* on a plasmid restored TS susceptibility to levels similar to those of the single *fpvA* mutant (**Table 1**). Together, these data suggest that TS exploits both pyoverdine receptors for entry.

TS is active against multi-drug resistant clinical isolates

To test whether TS could inhibit growth of a broader range of *P. aeruginosa* strains, particularly multi-drug resistant (MDR) isolates for which there are fewer antibiotic options, we tested 96 recent clinical isolates for susceptibility to TS in 10:90. While approximately 1 in 10 of those strains had an IC_{50} ≥5µM TS (**Fig 4A**), a combination of 5 µM TS (8.3 µg/ml) plus 86 µM DSX (32 µg/ml) reduced growth of all but three isolates of *P. aeruginosa* to less than 25% of the DMSO control (**Fig 4A**). We next tested the activity of TS against another MDR Gram-negative pathogen that can cause severe infections, *Acinetobacter baumanii* (38). *A. baumannii* strains encode FpvA and FpvB homologs (**Supplementary Fig S3**), suggesting they may be susceptible to the thiopeptide. Growth of 6 of 10 *A. baumannii* strains in 10:90 was reduced to ≤50% of control with 5 µM TS, while the combination of 5µM TS and 86 µM DSX reduced growth of 8/9 clinical isolates of *A. baumanii* below 10% of control (**Fig 4B**). As reported

previously (39), growth of *E. coli* – which lacks FpvAB homologs – was unaffected even at the maximum soluble concentration of 10 µM TS (not shown).

DISCUSSION

The natural role of antibiotics has been broadly debated (14, 16): are they signaling molecules that are toxic at high concentrations, or weapons used by bacteria to gain an advantage over competitors in their environment? The biofilm stimulation response to sub-inhibitory concentrations of antibiotics is consistent with both views. At concentrations too low to elicit damage, bacteria show little phenotypic response to antibiotic exposure. As concentrations approach the MIC, the bacteria respond in a dose-dependent manner by ramping up the amount of biofilm produced – detecting either the antibiotics or their effects – which may protect a subpopulation of cells. Above the MIC, antibiotics fall into the deadly weapons category. Biofilm stimulation by sub-inhibitory concentrations of antibiotics is a common phenomenon among multiple gram-positive and gram-negative species, and is caused by several drug classes, suggesting it is not necessarily linked to a specific MOA (16, 18, 40). As demonstrated here, this phenomenon can be used to identify potential antibiotic activity in the absence of killing, a useful feature when screening at a single arbitrary concentration that may be below the MIC for the drug-organism combination being tested. Interestingly, we and others (41) found that many drugs intended for eukaryotic targets can impact bacterial growth and biofilm formation (**Supplementary Table S1**), implying that they have deleterious effects on prokaryotic physiology. With a new appreciation of the role of the human microbiome in health and disease, these potential effects should be considered during drug development.

TS, a complex cyclic thiopeptide made by *Streptomyces azureus, S. hawaiiensis,* and *S. laurantii,* is experiencing a resurgence of research interest due to its broad anti-bacterial, anti-malarial, and anti-cancer activities (23, 24). It is a member of the RiPP (ribosomally synthesized and post-translationally modified peptides) class of natural products (42), derived from a 42-amino acid precursor, TsrA (43). Although the mechanism of its antibacterial activity (inhibition of translation by binding to helices H43/H44 of 23S rRNA) and resistance (methylation of 23S rRNA residue A1067) have been deciphered (26, 44), the way in which this ~1.7 kDa molecule enters target bacteria is unknown. Our data suggest that TS is actively imported into *P. aeruginosa* under iron-restricted conditions.

There are multiple examples of molecules that exploit iron uptake pathways to enter bacteria. Class I microcins – narrow-spectrum antibiotics produced by some gram negative species – bind to

siderophore receptors and share many of TS's properties. They are RiPPs, less than 5 kDa in mass, and cyclic (giving them the nickname 'lasso peptides'). Notably, binding of iron by microcins is not a prerequisite for uptake, as some interact with siderophore receptors in an iron-free state. For example, MccJ25, produced by *E. coli* (45), interacts with siderophore receptor FhuA by mimicking the structure of ferrichrome (46). It is not yet clear whether TS binds iron or simply mimics an iron-bound conformation, as it has multiple hydroxyls positioned in a manner that could coordinate metals (**Fig 1A**). Its structure has been solved both by X-ray crystallography and NMR, but no bound metals were reported (47, 48). The FpvA receptor is also exploited by S-pyocins, 40-80 kDa peptide antibiotics produced by competing *P. aeruginosa* strains, showing that it is a key promiscuous entry point for diverse molecules in addition to its usual ligand, pyoverdine (33, 34, 49).

Our discovery that TS exploits FpvA and FpvB for uptake into the periplasm helps to explain the resistance of gram-negative species such as *E. coli* to this antibiotic, as they lack those proteins. Bioinformatic searches show FpvAB homologs are expressed by *P. aeruginosa* and related pathogens – including *A. baumanii* (**Supplementary Fig S3**) – suggesting that TS could have utility as a narrow-spectrum agent. Use of multiple pyoverdine receptors by TS may reduce the probability of resistance arising through mutation of a single receptor, although genome analysis of clinical isolate C0379 that was most resistant to the combination of TS and DSX (**Fig 4A**) revealed a wild type copy of *fpvA* coupled with an ~800 bp deletion encompassing the 5' region of *fpvB*. Further investigation of *P. aeruginosa* strains that are resistant to TS will be needed to understand the most likely routes by which it occurs.

Although TS uses siderophore receptors to cross the *P. aeruginosa* OM, the way in which this large cyclic peptide transits the cytoplasmic membranes of gram-positive and gram-negative bacteria to reach its ribosomal targets remains undefined. Expression of *tsr* in *P. aeruginosa* conferred resistance, confirming that TS acts via its canonical bacteriostatic MOA. While PA14 expressing Tsr was significantly more resistant to TS than the control, it was more sensitive than PAO1. This difference is not due to nucleotide polymorphism at the Tsr methylation site on the rRNA, as these residues are conserved between PAO1 and PA14. The reasons for strain-specific differences in susceptibility are unclear, but our data confirm that most *P. aeruginosa* isolates tested (including MDR strains) are susceptible to TS, especially when it is combined with DSX (**Fig 4A, Supplementary Table S2**).

TS's major liability is its poor solubility (50). Smaller, more soluble fragments that retain activity against gram-positive bacteria and have reduced toxicity for eukaryotic cells have been identified (51) but it is not clear if they would be active against *P. aeruginosa* if uptake by the FpvAB receptors requires

the intact molecule. Another way to circumvent solubility issues is to reduce the required concentration. Our data show that this can be accomplished for TS by co-administration with FDA-approved iron chelators DFP or DSX (**Fig 3DE**). The true potential of TS as an anti-infective may be underestimated, as MIC evaluations are typically performed in rich, iron-replete media such as cation-adjusted Mueller-Hinton broth. Many host environments are iron-restricted, particularly in the presence of infection and inflammation (52-54) and future studies of TS activity should emulate those growth conditions.

In summary, we showed that biofilm stimulation can be used in high-throughput small molecule screening to report on sub-inhibitory antibiotic activity that may otherwise be missed using the usual metric of growth inhibition. In a small screen of less than 4000 molecules at a fixed concentration of 10 µM, we identified 60 molecules that stimulated biofilm formation, suggesting that they may have antimicrobial activity at higher concentrations, or under different growth conditions, as demonstrated here for TS. Stimulation of biofilm matrix production by TS in the gram-positive genus *Bacillus* was reported previously, and that phenotype leveraged to identify novel thiopeptide producers in co-cultures (55). Those studies, and the data presented here, suggest that monitoring biofilm stimulation (or an easily assayed proxy thereof, such as increased expression from biofilm matrix promoters) could allow for increased detection of molecules with potential antibacterial activity during screening, making it a useful addition to the antimicrobial discovery toolkit.

ACKNOWLEDGEMENTS

We thank Gerry Wright for access to strains from the Wright Clinical Collection, David Heinrichs for the gift of EDDHA and helpful discussions, and Neha Sharma, Andrew Hogan, Amanda Veri, and Victor Yang for assistance with method development. This work was supported by a Natural Sciences and Engineering Research (NSERC) grant RGPIN-2016-06521, and by Ontario Research Fund grant RE07-048. MRR and UN held Ontario Graduate Scholarships, MR was supported by an NSERC Undergraduate Summer Research Award, SKP was supported by a Summer Studentship from GlycoNet, and HA was supported by a Summer Studentship from Cystic Fibrosis Canada.

METHODS

Bacterial strains and culture conditions

The bacterial strains and plasmids used in this study are listed in **Table 1** and **Supplementary Table S2**. Bacterial cultures were grown in Lysogeny Broth (LB), 10:90 (10% LB and 90% phosphate buffered

saline), M9 medium, Vogel Bonner minimal medium (VBMM), or cation-adjusted Mueller-Hinton broth (MBH) as indicated. Where solid media were used, plates were solidified with 1.5% agar. DFP (Sigma-Aldrich) and DSX (Cayman Chemicals) were stored at 4°C until use. TS was stored at -20˚C. A 60 mg/mL stock solution of DFP was made in 6M HCl and Milli-Q H_2O (DFP solvent) in a ratio of 3:50. A 20 mg/mL stock solution of DSX was made in DMSO. A 20mM stock solution of TS was made in DMSO.

Growth curves

PAO1-KP was inoculated from a -80°C stock into 5 ml LB broth and grown with shaking at 200 rpm, 16h, 37°C. The overnight culture was subcultured at 1:500 into 5 different media (LB, 10:90, M9, Mueller-Hinton (MH), and VBMM) – incubated at 37°C for 6h with shaking at 200 rpm. Each subculture was standardized to OD_{600} ~ 0.1 (Biomate 3 Spectrophotometer) then diluted 1:500 into the same medium. Six replicates of 200 µl of each sample were added to a 96 well plate, which was incubated at 37°C for 24 h with shaking at 200 rpm (Tecan Ultra Evolution plate reader). The OD_{612} was read every 15 min for 24 h. The data for the six replicates of each sample were averaged and the experiment was repeated 3 times. The final data with standard deviations were plotted using Prism (Graphpad).

Biofilm modulation assay

Biofilm formation was assayed as described in (11), with modifications. Briefly, *P. aeruginosa* was inoculated in 5 mL of LB and grown at 37°C overnight, shaking at 200 rpm, and subsequently standardized to an OD_{600} of ~ 0.1 in 10:90. For the initial screen, 1 mM compound stocks in DMSO were diluted 1:100 in standardized cell suspension (1.5 µL of compound stock in 148.5 µL of cell suspension) to a final concentration of 10 µM. Control wells contained 10:90 plus 1% DMSO (sterility control) or standardized cell suspension plus 1% DMSO (growth control). Biofilms were formed on polystyrene peg lids (Nunc). After placement of the peg lid, the plate was sealed with parafilm to prevent evaporation and incubated for 16 h at 37°C, 200 rpm. Following incubation, the 96-peg lid was removed and planktonic density in the 96 well plate measured at OD_{600} to assess the effect of test compounds on bacterial growth. The lid was transferred to a new microtiter plate containing 200 µl of 1X phosphate-buffered saline (PBS) per well for 10 min to wash off any loosely adherent bacterial cells, then to a microtiter plate containing 200 µL of 0.1% (wt/vol) CV per well for 15 min. Following staining, the lid was washed with 70 mL of dH_2O, in a single well tray, for 10 min. This step was repeated four times to ensure complete removal of excess CV. The lid was transferred to a 96-well plate containing 200 µL of 33% (vol/vol) acetic acid per well for 5 min to elute the bound CV. The absorbance of the eluted CV was

286 measured at 600 nm (BioTek ELx800), and the results plotted as percent of the DMSO control using
287 Prism (Graphpad). Screens were performed in duplicate. Compounds that resulted in <50% of control
288 biofilm were defined as biofilm inhibitors, while compounds that resulted in >200% of control biofilm
289 were defined as biofilm stimulators. Compounds of interest were further evaluated using the same
290 assay but over a wider range of concentrations (dose-response assay).

291 For TS dose response assays, TS stock solutions were diluted in DMSO and 2µL of the resulting
292 solutions plus 148µL of a bacterial suspension standardized to an OD_{600} of ~ 0.1 in 10:90 were added to a
293 96 well plate in triplicate, as described above. Control wells contained 148µL of 10:90 + 1.3% DMSO
294 (sterility control) or standardized bacterial suspension + 1.3% DMSO (growth control). For EDDHA alone
295 or with $FeCl_3$ experiments, 2µL of each were added as aqueous solutions to reach final concentrations of
296 0.1µM EDDHA and 100µM $FeCl_3$, and the amount of bacterial suspension adjusted to keep the total well
297 volume at 150µL. Controls for EDDHA and $FeCl_3$ were 2µL of sterile dH_20. Biofilms were grown for 16h at
298 37˚C, 200 rpm, then stained and quantified as described above. Assays were performed in triplicate and
299 results were graphed using Prism (Graphpad) as a percentage of the DMSO control.

300 **Compounds screened**

301 The biofilm modulation assay was used to screen the McMaster Bioactives compound
302 collection. This curated collection includes off-patent, FDA-approved drugs from the Prestwick Chemical
303 Library (Prestwick Chemical, Illkirch, France), purified natural products from the Screen-Well Natural
304 Products Library (Enzo Life Sciences, Inc., Farmingdale, NY, USA), drug-like molecules from the
305 Lopac^{1280} (International Version) collection (Sigma-Aldrich Canada Ltd., Oakville, ON, Canada) and the
306 Spectrum Collection (MicroSource Discovery Systems, Inc., Gaylordsville, CT, USA) which includes off
307 patent drugs, natural products, and other biologically active compounds. In total, the collection is 3921
308 unique compounds.

309 **Construction of a *tsr* plasmid for expression in *P. aeruginosa***

310 The *tsr* gene from pIJ6902 (56) was PCR-amplified using primers
311 5' GAATCCCGGGCGGTAGGACGACCATGAC 3' and 5' CTTCAAGCTTTTATCGGTTGGCCGCGAG 3'. Both the
312 PCR product and pUCP20 vector were digested with SmaI and HindIII, gel-purified, and ligated at a 1:3
313 molar ratio using T4 DNA ligase. The ligated DNA was transformed into *E. coli* DH5a and transformants
314 selected on LB agar containing 100 µg/mL ampicillin and 5-bromo-4-chloro-3-indolyl-β-D-
315 galactopyranoside for blue-white selection. Plasmids from white colonies were purified using a GeneJet

Plasmid Miniprep kit (Thermo Scientific) following the manufacturer's protocols. After verification by restriction digest and DNA sequencing, pUCP20 and pUCP20-tsr were each introduced into *P. aeruginosa* PAO1 and PA14 by electroporation. Transformants were selected on LB agar containing 200 µg/mL carbenicillin.

IC_{50} and checkboard assays

IC_{50} values were determined with microbroth dilution assays in Nunc 96-well plates. Vehicle controls consisted of 1:75 dilutions of DMSO in 10:90 inoculated with PA14 or its mutants as described in Growth Curves. Sterile controls consisted of 1:75 dilutions of DMSO in 10:90. Seven serially diluted concentrations of TS – with 17 µg/mL being the highest final concentration – was set up in triplicate. Tests were done with 1:75 dilutions of each TS concentration in 10:90 inoculated with PA14 or its mutants as described in Growth Curves. Plates were sealed to prevent evaporation and incubated with shaking at 200 rpm, 16h, 37°C. The OD_{600} of the plates was read (Multiskan Go - Thermo Fisher Scientific) and used to calculate IC_{50}. The final volume of each well was 150 µL and each experiment was repeated at least three times.

Checkerboard assays were set-up using Nunc 96-well plates in an 8-well by 8-well format. Two columns were allocated for vehicle controls and two columns for sterility controls. Vehicle controls contained 2 µL DMSO + 2 µL DFP solvent for checkerboards with TS and DFP or 4 µL DMSO for TS and DSX, in 146 µL of 10:90 inoculated with PA14 or PAO1-KP as described in Growth Curves. Sterile controls contained the same components in 10:90, without cells. Serial dilutions of TS – with 17 µg/mL being the highest final concentration – was added along the ordinate of the checkerboard (increasing concentration from bottom to top) whereas serial dilutions of DFP or DSX – with 512 µg/mL being the highest final concentration – was added along the abscissa (increasing concentration from left to right). The final volume of each well was 150 µL and each checkerboard was repeated at least three times. Plates were incubated and the final OD_{600} determined as detailed above.

Clinical isolates testing

Clinical isolates of *P. aeruginosa* and *A. baumannii* were inoculated from -80°C stocks into 200 µL LB broth and grown with shaking at 200 rpm, 16h, 37°C. in Nunc 96-well plates. The overnight cultures were subcultured (1:25 dilution) into 10:90 and grown with shaking at 200 rpm, 2h, 37°C**.** Vehicle controls consisted of 4 µL of DMSO, 144µL 10:90 and 2 µL of subculture. Sterile controls consisted of 4 µL of DMSO and 146µL 10:90. Test samples consisted of 2 µL of TS (final concentration of 5 µM, 8.3

346 µg/ml), 2 µL of DMSO (or DSX, final concentration of 86 µM, 32 µg/mL), 144 µL 10:90 and 2 µL of
347 subculture. The final volume of each well was 150 µL and each checkerboard was repeated at least three
348 times. Plates were incubated with shaking at 200 rpm, 16h, 37°C and OD_{600} was measured (Multiskan Go
349 - Thermo Fisher Scientific). The results were plotted as percent of control (wells containing only DMSO)
350 using Prism (GraphPad).

351 **REFERENCES**

352 1. Zabawa TP, Pucci MJ, Parr TR, Jr., Lister T. 2016. Treatment of Gram-negative bacterial infections
353 by potentiation of antibiotics. Curr Opin Microbiol 33:7-12.
354 2. Blair JM, Webber MA, Baylay AJ, Ogbolu DO, Piddock LJ. 2015. Molecular mechanisms of
355 antibiotic resistance. Nat Rev Microbiol 13:42-51.
356 3. Hall CW, Mah TF. 2017. Molecular mechanisms of biofilm-based antibiotic resistance and
357 tolerance in pathogenic bacteria. FEMS Microbiol Rev 41:276-301.
358 4. Kalan L, Wright GD. 2011. Antibiotic adjuvants: multicomponent anti-infective strategies. Expert
359 Rev Mol Med 13:e5.
360 5. Tacconelli E, Carrara E, Savoldi A, Harbarth S, Mendelson M, Monnet DL, Pulcini C, Kahlmeter G,
361 Kluytmans J, Carmeli Y, Ouellette M, Outterson K, Patel J, Cavaleri M, Cox EM, Houchens CR,
362 Grayson ML, Hansen P, Singh N, Theuretzbacher U, Magrini N, Group WHOPPLW. 2018.
363 Discovery, research, and development of new antibiotics: the WHO priority list of antibiotic-
364 resistant bacteria and tuberculosis. Lancet Infect Dis 18:318-327.
365 6. Fothergill JL, Winstanley C, James CE. 2012. Novel therapeutic strategies to counter
366 *Pseudomonas aeruginosa* infections. Expert Rev Anti Infect Ther 10:219-35.
367 7. Rybtke M, Hultqvist LD, Givskov M, Tolker-Nielsen T. 2015. *Pseudomonas aeruginosa* Biofilm
368 Infections: Community Structure, Antimicrobial Tolerance and Immune Response. J Mol Biol
369 427:3628-45.
370 8. Burrows LL. 2018. The Therapeutic Pipeline for *Pseudomonas aeruginosa* Infections. ACS Infect
371 Dis 4:1041-1047.
372 9. Nguyen L, Garcia J, Gruenberg K, MacDougall C. 2018. Multidrug-Resistant *Pseudomonas*
373 Infections: Hard to Treat, But Hope on the Horizon? Curr Infect Dis Rep 20:23.
374 10. Page MG, Heim J. 2009. Prospects for the next anti-*Pseudomonas* drug. Curr Opin Pharmacol
375 9:558-65.

11. Wenderska IB, Chong M, McNulty J, Wright GD, Burrows LL. 2011. Palmitoyl-DL-carnitine is a multitarget inhibitor of *Pseudomonas aeruginosa* biofilm development. Chembiochem 12:2759-66.

12. Ejim L, Farha MA, Falconer SB, Wildenhain J, Coombes BK, Tyers M, Brown ED, Wright GD. 2011. Combinations of antibiotics and nonantibiotic drugs enhance antimicrobial efficacy. Nat Chem Biol 7:348-50.

13. Hoffman LR, D'Argenio DA, MacCoss MJ, Zhang Z, Jones RA, Miller SI. 2005. Aminoglycoside antibiotics induce bacterial biofilm formation. Nature 436:1171-5.

14. Linares JF, Gustafsson I, Baquero F, Martinez JL. 2006. Antibiotics as intermicrobial signaling agents instead of weapons. Proc Natl Acad Sci U S A 103:19484-9.

15. Jones C, Allsopp L, Horlick J, Kulasekara H, Filloux A. 2013. Subinhibitory concentration of kanamycin induces the *Pseudomonas aeruginosa* type VI secretion system. PLoS One 8:e81132.

16. Oliveira NM, Martinez-Garcia E, Xavier J, Durham WM, Kolter R, Kim W, Foster KR. 2015. Biofilm Formation As a Response to Ecological Competition. PLoS Biol 13:e1002191.

17. Ahmed MN, Porse A, Sommer MOA, Hoiby N, Ciofu O. 2018. Evolution of Antibiotic Resistance in Biofilm and Planktonic *Pseudomonas aeruginosa* Populations Exposed to Subinhibitory Levels of Ciprofloxacin. Antimicrob Agents Chemother 62.

18. Ranieri MR, Whitchurch CB, Burrows LL. 2018. Mechanisms of biofilm stimulation by subinhibitory concentrations of antimicrobials. Curr Opin Microbiol 45:164-169.

19. Delcour AH. 2009. Outer membrane permeability and antibiotic resistance. Biochim Biophys Acta 1794:808-16.

20. Cox G, Wright GD. 2013. Intrinsic antibiotic resistance: mechanisms, origins, challenges and solutions. Int J Med Microbiol 303:287-92.

21. Zlitni S, Ferruccio LF, Brown ED. 2013. Metabolic suppression identifies new antibacterial inhibitors under nutrient limitation. Nat Chem Biol 9:796-804.

22. Weisblum B, Demohn V. 1970. Thiostrepton, an inhibitor of 5OS ribosome subunit function. J Bacteriol 101:1073-5.

23. Gartel AL. 2008. FoxM1 inhibitors as potential anticancer drugs. Expert Opin Ther Targets 12:663-5.

24. Aminake MN, Schoof S, Sologub L, Leubner M, Kirschner M, Arndt HD, Pradel G. 2011. Thiostrepton and derivatives exhibit antimalarial and gametocytocidal activity by dually targeting parasite proteasome and apicoplast. Antimicrob Agents Chemother 55:1338-48.

25. Bibb MJ, Bibb MJ, Ward JM, Cohen SN. 1985. Nucleotide sequences encoding and promoting expression of three antibiotic resistance genes indigenous to Streptomyces. Mol Gen Genet 199:26-36.

26. Dunstan MS, Hang PC, Zelinskaya NV, Honek JF, Conn GL. 2009. Structure of the thiostrepton resistance methyltransferase.S-adenosyl-L-methionine complex and its interaction with ribosomal RNA. J Biol Chem 284:17013-20.

27. Sezonov G, Joseleau-Petit D, D'Ari R. 2007. Escherichia coli physiology in Luria-Bertani broth. J Bacteriol 189:8746-9.

28. Vogel HJ, Bonner DM. 1956. Acetylornithinase of Escherichia coli: partial purification and some properties. J Biol Chem 218:97-106.

29. Pletzer D, Braun Y, Dubiley S, Lafon C, Kohler T, Page MGP, Mourez M, Severinov K, Weingart H. 2015. The Pseudomonas aeruginosa PA14 ABC Transporter NppA1A2BCD Is Required for Uptake of Peptidyl Nucleoside Antibiotics. J Bacteriol 197:2217-2228.

30. Pletzer D, Braun Y, Weingart H. 2016. Swarming motility is modulated by expression of the putative xenosiderophore transporter SppR-SppABCD in *Pseudomonas aeruginosa* PA14. Antonie Van Leeuwenhoek 109:737-53.

31. Grinter R, Milner J, Walker D. 2013. Beware of proteins bearing gifts: protein antibiotics that use iron as a Trojan horse. FEMS Microbiol Lett 338:1-9.

32. Braun V, Pramanik A, Gwinner T, Koberle M, Bohn E. 2009. Sideromycins: tools and antibiotics. Biometals 22:3-13.

33. Denayer S, Matthijs S, Cornelis P. 2007. Pyocin S2 (Sa) kills *Pseudomonas aeruginosa* strains via the FpvA type I ferripyoverdine receptor. J Bacteriol 189:7663-8.

34. Elfarash A, Wei Q, Cornelis P. 2012. The soluble pyocins S2 and S4 from *Pseudomonas aeruginosa* bind to the same FpvAI receptor. Microbiologyopen 1:268-75.

35. Poole K, Neshat S, Heinrichs D. 1991. Pyoverdine-mediated iron transport in *Pseudomonas aeruginosa*: involvement of a high-molecular-mass outer membrane protein. FEMS Microbiol Lett 62:1-5.

36. Kwiatkowski JL. 2016. Current recommendations for chelation for transfusion-dependent thalassemia. Ann N Y Acad Sci 1368:107-14.

37. Liberati NT, Urbach JM, Miyata S, Lee DG, Drenkard E, Wu G, Villanueva J, Wei T, Ausubel FM. 2006. An ordered, nonredundant library of *Pseudomonas aeruginosa* strain PA14 transposon insertion mutants. Proc Natl Acad Sci U S A 103:2833-8.

38. Harding CM, Hennon SW, Feldman MF. 2018. Uncovering the mechanisms of *Acinetobacter baumannii* virulence. Nat Rev Microbiol 16:91-102.

39. Singer ME, Finnerty WR. 1988. Construction of an *Escherichia coli-Rhodococcus* shuttle vector and plasmid transformation in *Rhodococcus* spp. J Bacteriol 170:638-45.

40. Townsley L, Shank EA. 2017. Natural-Product Antibiotics: Cues for Modulating Bacterial Biofilm Formation. Trends Microbiol 25:1016-1026.

41. Maier L, Pruteanu M, Kuhn M, Zeller G, Telzerow A, Anderson EE, Brochado AR, Fernandez KC, Dose H, Mori H, Patil KR, Bork P, Typas A. 2018. Extensive impact of non-antibiotic drugs on human gut bacteria. Nature 555:623-628.

42. Arnison PG, Bibb MJ, Bierbaum G, Bowers AA, Bugni TS, Bulaj G, Camarero JA, Campopiano DJ, Challis GL, Clardy J, Cotter PD, Craik DJ, Dawson M, Dittmann E, Donadio S, Dorrestein PC, Entian KD, Fischbach MA, Garavelli JS, Goransson U, Gruber CW, Haft DH, Hemscheidt TK, Hertweck C, Hill C, Horswill AR, Jaspars M, Kelly WL, Klinman JP, Kuipers OP, Link AJ, Liu W, Marahiel MA, Mitchell DA, Moll GN, Moore BS, Muller R, Nair SK, Nes IF, Norris GE, Olivera BM, Onaka H, Patchett ML, Piel J, Reaney MJ, Rebuffat S, Ross RP, Sahl HG, Schmidt EW, Selsted ME, et al. 2013. Ribosomally synthesized and post-translationally modified peptide natural products: overview and recommendations for a universal nomenclature. Nat Prod Rep 30:108-60.

43. Kelly WL, Pan L, Li C. 2009. Thiostrepton biosynthesis: prototype for a new family of bacteriocins. J Am Chem Soc 131:4327-34.

44. Baumann S, Schoof S, Bolten M, Haering C, Takagi M, Shin-ya K, Arndt HD. 2010. Molecular determinants of microbial resistance to thiopeptide antibiotics. J Am Chem Soc 132:6973-81.

45. Asensio C, Perez-Diaz JC. 1976. A new family of low molecular weight antibiotics from enterobacteria. Biochem Biophys Res Commun 69:7-14.

46. Mathavan I, Zirah S, Mehmood S, Choudhury HG, Goulard C, Li Y, Robinson CV, Rebuffat S, Beis K. 2014. Structural basis for hijacking siderophore receptors by antimicrobial lasso peptides. Nat Chem Biol 10:340-2.

47. Anderson B, Hodgkin DC, Viswamitra MA. 1970. The structure of thiostrepton. Nature 225:233-5.

48. Jonker HR, Baumann S, Wolf A, Schoof S, Hiller F, Schulte KW, Kirschner KN, Schwalbe H, Arndt HD. 2011. NMR structures of thiostrepton derivatives for characterization of the ribosomal binding site. Angew Chem Int Ed Engl 50:3308-12.

471 49. White P, Joshi A, Rassam P, Housden NG, Kaminska R, Goult JD, Redfield C, McCaughey LC,
472 Walker D, Mohammed S, Kleanthous C. 2017. Exploitation of an iron transporter for bacterial
473 protein antibiotic import. Proc Natl Acad Sci U S A 114:12051-12056.
474 50. Zhang F, Kelly WL. 2012. In vivo production of thiopeptide variants. Methods Enzymol 516:3-24.
475 51. Nicolaou KC, Zak M, Rahimipour S, Estrada AA, Lee SH, O'Brate A, Giannakakou P, Ghadiri MR.
476 2005. Discovery of a biologically active thiostrepton fragment. J Am Chem Soc 127:15042-4.
477 52. Schaible UE, Kaufmann SH. 2004. Iron and microbial infection. Nat Rev Microbiol 2:946-53.
478 53. Nairz M, Schroll A, Sonnweber T, Weiss G. 2010. The struggle for iron - a metal at the host-
479 pathogen interface. Cell Microbiol 12:1691-702.
480 54. Cassat JE, Skaar EP. 2013. Iron in infection and immunity. Cell Host Microbe 13:509-519.
481 55. Bleich R, Watrous JD, Dorrestein PC, Bowers AA, Shank EA. 2015. Thiopeptide antibiotics
482 stimulate biofilm formation in *Bacillus subtilis*. Proc Natl Acad Sci U S A 112:3086-91.
483 56. Huang J, Shi J, Molle V, Sohlberg B, Weaver D, Bibb MJ, Karoonuthaisiri N, Lih CJ, Kao CM,
484 Buttner MJ, Cohen SN. 2005. Cross-regulation among disparate antibiotic biosynthetic pathways
485 of *Streptomyces coelicolor*. Mol Microbiol 58:1276-87.

486

487

488 **Table 1.** Susceptibility of *P. aeruginosa* mutants to thiostrepton in VBMM.

Strain	Gene	Function	IC_{50} µg/ml	IC_{50} µM
PA14	N/A	Wild type strain	0.26	0.16
fpvA::Mar2xT7	PA2398	Type 1 ferripyoverdine receptor	3.68	2.21
fpvB::Mar2xT7	PA4168	Alternate Type 1 ferripyoverdine receptor	1.83	1.10
pvdA::Mar2xT7	PA2386	L-ornithine N5-oxygenase	0.26	0.16
Δ*fpvA* *fpvB*::Mar2xT7	PA2398, PA4168	Type I ferripyoverdine receptor, Alternate type I ferripyoverdine receptor	6.93	4.16
Δ*fpvA* *fpvB*::Mar2xT7 + pUCP20	PA2398, PA4168	Type I ferripyoverdine receptor, Alternate type I ferripyoverdine receptor	4.20	2.52
Δ*fpvA* *fpvB*::Mar2xT7 + pUCP20-*fpvB*	PA2398, PA4168	Type I ferripyoverdine receptor, Alternate type I ferripyoverdine receptor	2.80	1.68
fptA::Mar2xT7	PA4221	Pyochelin receptor	0.26	0.16
PA1322::Mar2xT7	PA1322	Probable TonB-dependent receptor	0.26	0.16
PA4837::Mar2xT7	PA4837	Probable outer membrane protein precursor	0.26	0.16
foxA::Mar2xT7	PA2466	Ferrioxamine receptor FoxA	0.26	0.16
fiuA::Mar2xT7	PA0470	Ferrichrome receptor FiuA	0.26	0.16
pirA::Mar2xT7	PA0931	Alternate enterobactin receptor	0.35	0.21
pfeA::Mar2xT7	PA2688	Enterobactin receptor	0.26	0.16
hasR::Mar2xT7	PA3408	Heme uptake outer membrane receptor	0.35	0.21
fvbA::Mar2xT7	PA4516	Vibriobactin receptor	0.26	0.16
piuA::Mar2xT7	PA4514	Hydroxamate-type ferrisiderophore receptor	0.35	0.21
PA0151::Mar2xT7	PA0151	Probable TonB-dependent receptor	0.26	0.16

chtA::Mar2xT7	PA4675	Aerobactin, Rhizobactin 1021, Schizokinen receptor	0.59	0.36
phuR::Mar2xT7	PA4710	Heme/Hemoglobin uptake receptor precursor	0.26	0.16

489

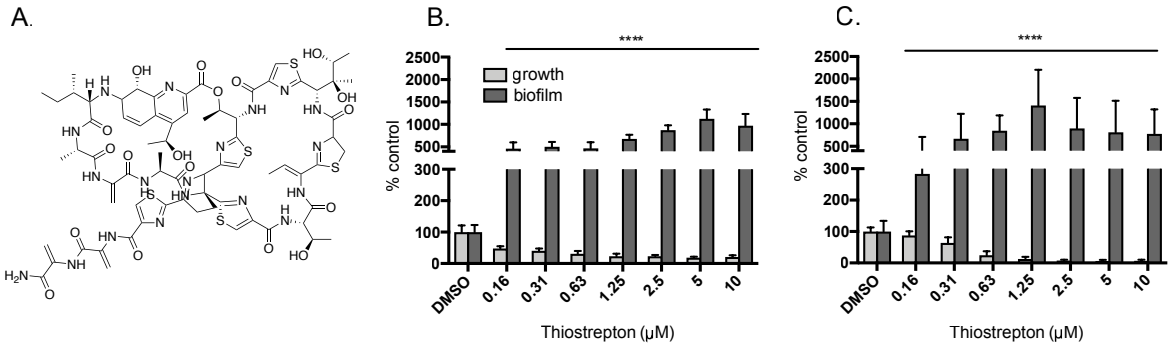

Figure 1. Thiostrepton stimulates *P. aeruginosa* biofilm formation. A. Structure of thiostrepton (TS). **B.** TS stimulated biofilm formation (absorbance of eluted crystal violet at 600 nm, plotted as percent of the DMSO control) of *P. aeruginosa* PAO1 and decreased planktonic cell density (optical density at 600 nm, plotted as percent of the DMSO control) in 10:90 medium in a dose-dependent manner, up to its maximum soluble concentration of 10 μM (17 μg/ml). **C.** In VBMM, PAO1 biofilm formation was stimulated by TS, while planktonic cell density decreased below the level of detection at concentrations above 1.25 μM. Y-axes are split to better display growth values. Assays were performed at least 3 times in triplicate. **** p<0.0001

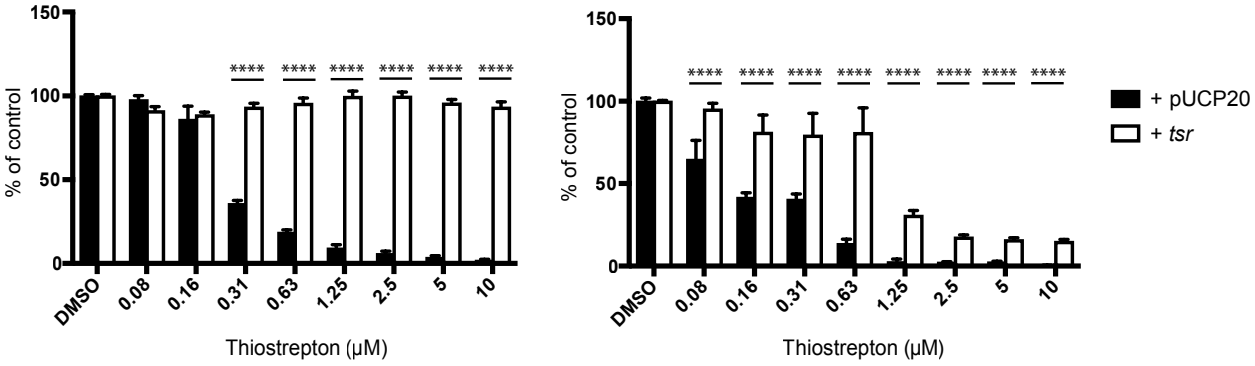

Figure 2. Expression of Tsr in trans reduces susceptibility of *P. aeruginosa* to thiostrepton. Expression of the *tsr* gene from *Streptomyces azureus* in trans from pUCP20 in two strains of *P. aeruginosa* reduced their susceptibility to TS in VBMM, suggesting it inhibits growth via its canonical mode of action, disrupting translation. **A.** Growth of PAO1 (OD_{600} plotted as percent of the DMSO control); **B.** Growth of PA14. Each assay was performed at least 3 times in triplicate. **** p<0.0001

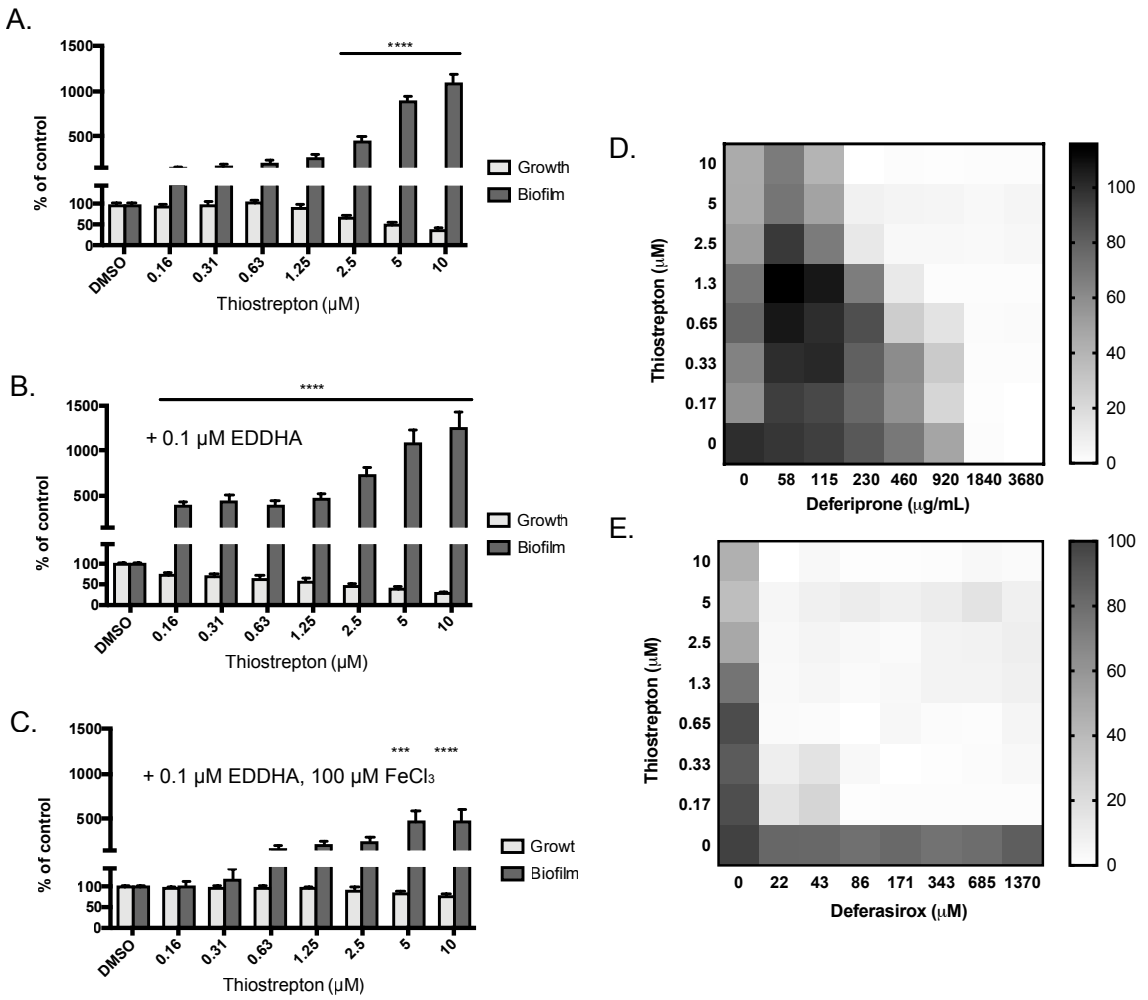

506

507 **Figure 3. Thiostrepton activity is potentiated by iron chelators.** Biofilm stimulation by TS in 10:90
508 medium increased in the presence of 0.1 μM EDDHA, a cell-impermeant iron chelator, while further
509 addition of 100 μM $FeCl_3$ increased the concentration of TS required for biofilm stimulation and growth
510 inhibition. **A.** PAO1 growth (OD_{600}) and biofilm (absorbance of CV at 600 nm) in 10:90 medium alone; **B.**
511 10:90 plus 0.1μM EDDHA; **C.** 10:90 plus 0.1μM EDDHA and 100 μM $FeCl_3$. Checkerboard assays plotted
512 as percent growth of the DMSO control (0,0 μM at lower left) showed that TS activity against PAO1 was
513 potentiated by FDA-approved iron chelators, **D.** deferiprone and **E.** deferasirox. The highest
514 concentrations of DFP (3680 μM) and DSX (1370 μM) are each equal to 512 μg/ml. Each assay was
515 performed at least 3 times. *** p<0.001; **** p<0.0001

516

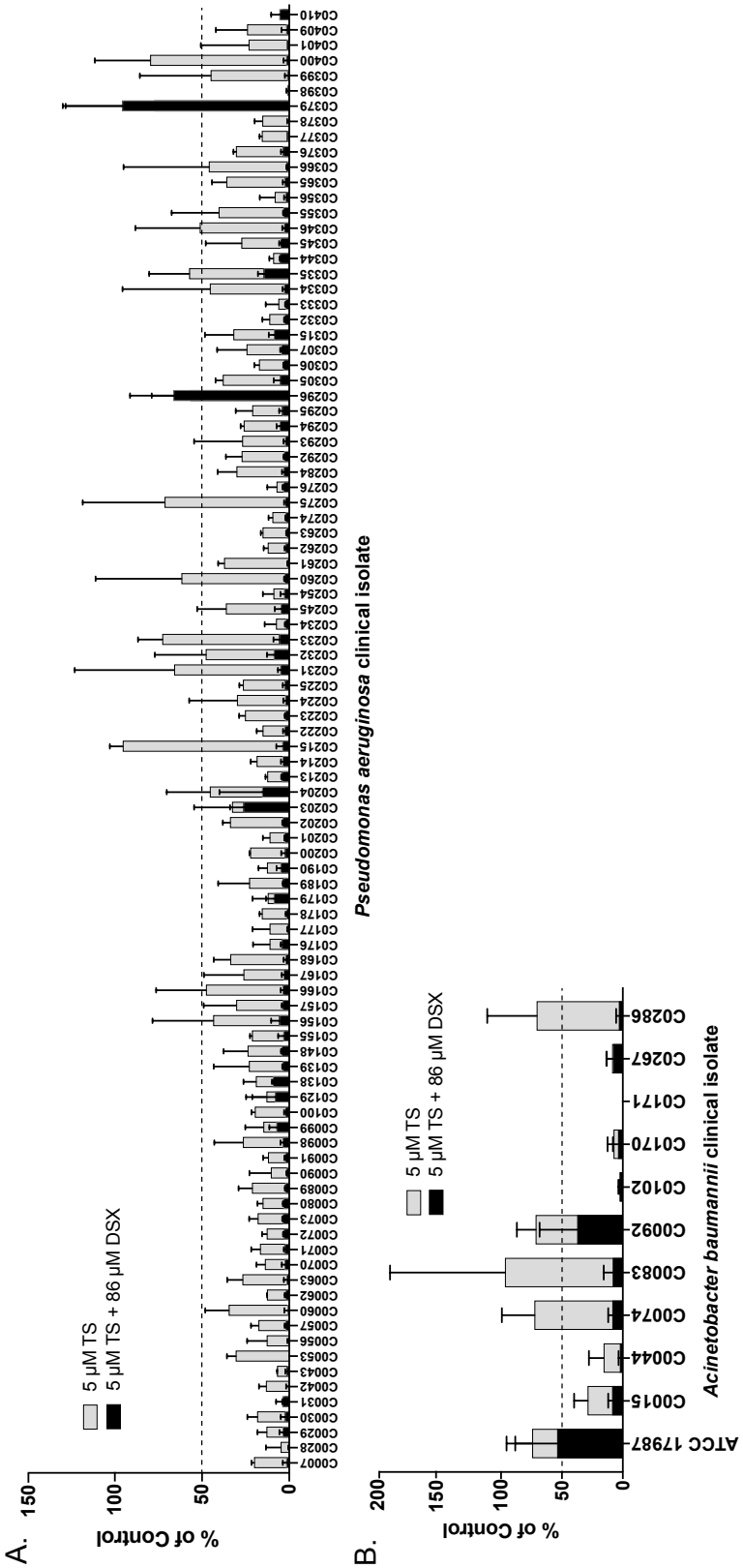

517

518 **Figure 4. Thiostrepton inhibits growth of multidrug-resistant clinical isolates.** The growth of most
519 clinical isolates of **A.** *P. aeruginosa* and **B.** *Acinetobacter baumannii* resistant to multiple antibiotics (see
520 **Supplementary Table S2** for antibiograms) was inhibited by 5 μM (8.3 μg/ml) TS in 10:90 medium (grey
521 bars). TS activity was potentiated by the addition of 86 μM deferasirox (DSX; 32 μg/ml; black bars). Each
522 assay was performed at least 3 times and the results plotted as percent of the DMSO-only growth
523 control (OD_{600}) using Prism (GraphPad). Error bars equal one standard deviation.